# Long-chain alkenone unsaturation index as sea surface temperature proxy in southwest Bay of Bengal

**Nittala S. Sarma[1,*], Sk. G. Pasha[1], M. Sri Rama Krishna[1], P. V. Shirodkar[2], M. G. Yadava[3] and K. Mohan Rao[4]**

[1]School of Chemistry, Andhra University, Visakhapatnam 530 003, India
[2]Chemical Oceanography Division, National Institute of Oceanography, Dona Paula, Goa 403 004, India
[3]Physical Research Laboratory, Navrangpura, Ahmedabad 380 009, India
[4]NIO Regional Centre, 51 Lawsons Bay Colony, Visakhapatnam 530 017, India

**As a proxy of the sea surface temperature (SST), $C_{37}$ long-chain alkenones (LCAs) preserved in sediments of the southwestern Bay of Bengal and dating back to the last glacial period, were identified in SIM GC-EI MS spectra run at *m/z* 530.55 (dienone: $C_{37:2}$ LCA) and 528.52 (trienone: $C_{37:3}$ LCA). The yields of LCAs ($C_{37:2}$ + $C_{37:3}$) relative to extractable lipid of the sediment are higher in the glacial than the Holocene sediments by a factor of three. The LCA unsaturation index ($U^{k'}_{37}$) and the SST calculated from calibration equations showed coherence with $\delta^{18}O$ of the planktonic foraminifer, *Globigerinoides ruber*. It is inferred that with reference to the Holocene, the last glacial surface sea water was ~ 2.75°C cooler from the alkenone data and was ~ 2‰ more saline from a combination of LCA and $\delta^{18}O$ data.**

**Keywords:** Holocene, long-chain alkenones, SW Bay of Bengal, sea surface temperature, unsaturation index.

FOR India, essentially an agro-based economy, stakes are high in the understanding of monsoon intensity and monsoon dynamics, on which the agricultural production depends. Knowledge of past variability of monsoon can provide clues to the present and future scenarios. The monsoon intensity is intimately connected to sea surface temperature (SST). The intensity of palaeomonsoon can be inferred from palaeo-SST, itself modulated by the glacial–interglacial cycles. The palaeo-SST can be inferred from various proxies in undisturbed ocean sediments. The widely used inorganic geochemical proxies are $\delta^{18}O$ of the surface-dwelling planktonic foraminiferal test calcite[1], and its Mg/Ca ratio[2]. The bulk sediment organic geochemical proxy of long-chain alkenones (LCA) is one of the actively pursued proxies in recent times[3].

Surface-dwelling prymnesiophyte microalgae, e.g. *Emiliana huxleyi* and *Gephyrocapsa oceanica* produce a suite of LCAs, whose molecular unsaturation is dependent on the temperature at which they carry out photosynthesis. Broadly speaking, lower the temperature, higher is the concentration of *ca.* triunsaturated LCA ($C_{37:3}$) relative to the diunsaturated LCA ($C_{37:2}$) that were observed. It is fortuitous that the concentrations of these LCAs relative to each other, from the time of their biosynthesis in the living plant cells remain the same[4], even after the death of the plant cells and through sedimentary diagenesis during which time a large fraction of bulk organic matter undergoes degradative loss. This is because structurally, the LCAs have long methylene chains in which the unsaturation is deeply embedded, and hence exerts little influence on oxidation, although the trienone should in principle be expected to undergo a preferential loss over the dienone[5]. The *E* stereochemistry, contrary to the usually noticed *Z* stereochemistry in natural compounds enables stabilization of molecules by a loose bonding across layers within the $CaCO_3$ matrix. The LCA unsaturation index ($U^{k'}_{37}$) defined by eq. (1)[6] is a new proxy that is frequently analysed at present globally, as the index does not suffer from disadvantages associated with other methods, e.g. melt water[1] and salinity effects[7] in the case of $\delta^{18}O$ and in the case of Mg/Ca, the water depth (i.e. temperature) at which (secondary) calcification of the foraminifer occurs in its late life cycle[2].

$$U^{k'}_{37} = \frac{[C_{37:2}]}{[C_{37:2}] + [C_{37:3}]} \quad (1)$$

Taking Indian marginal sediments as test samples, we have attempted to introduce new methodologies for investigating oceanic phenomena. As part of this, we have recently shown[8] the utility of amino acid racemization as a stratigraphic tool in core sediments raised at 78°35′E, 8°05.090′N in SW Bay of Bengal. Working on the same core sediments, we now report the methodology and results of LCA unsaturation index and its utility as a palaeo-SST proxy.

Well-preserved, frozen, dry sediment powders (15 g each) were soxhlett extracted in two steps: (i) ethyl acetate-hexane (1 : 9) and (ii) chloroform-methanol (3 : 1). Residue from the combined extract taken in *n*-hexane was passed through a small bed of Cu powder (to remove free S and its compounds), and the residue thereof saponified under nitrogen with 0.1 M KOH in methanol : water (90 : 10, 0.3 ml) at 80°C in a capped vial[9] for 2 h. From the cooled solutions, lipid components were partitioned into chloroform. Residues thereof were again chromatographed on silica gel column (6 mm id, 3 g). The first elution was done with *n*-hexane (20 ml) and the second with 2% EtOAc (20 ml; in *n*-hexane). Residue from the latter fraction, dissolved in 10% EtOAc (in hexane; 50–100 µl) was injected onto the gas chromatography (GC) (HP 6890) column (1 µl, 2 : 1 split). The extraction and purification procedure could be applied routinely for a large throughput of samples, and it incorporates the important

*For correspondence. (e-mail: nittalas@lycos.com)

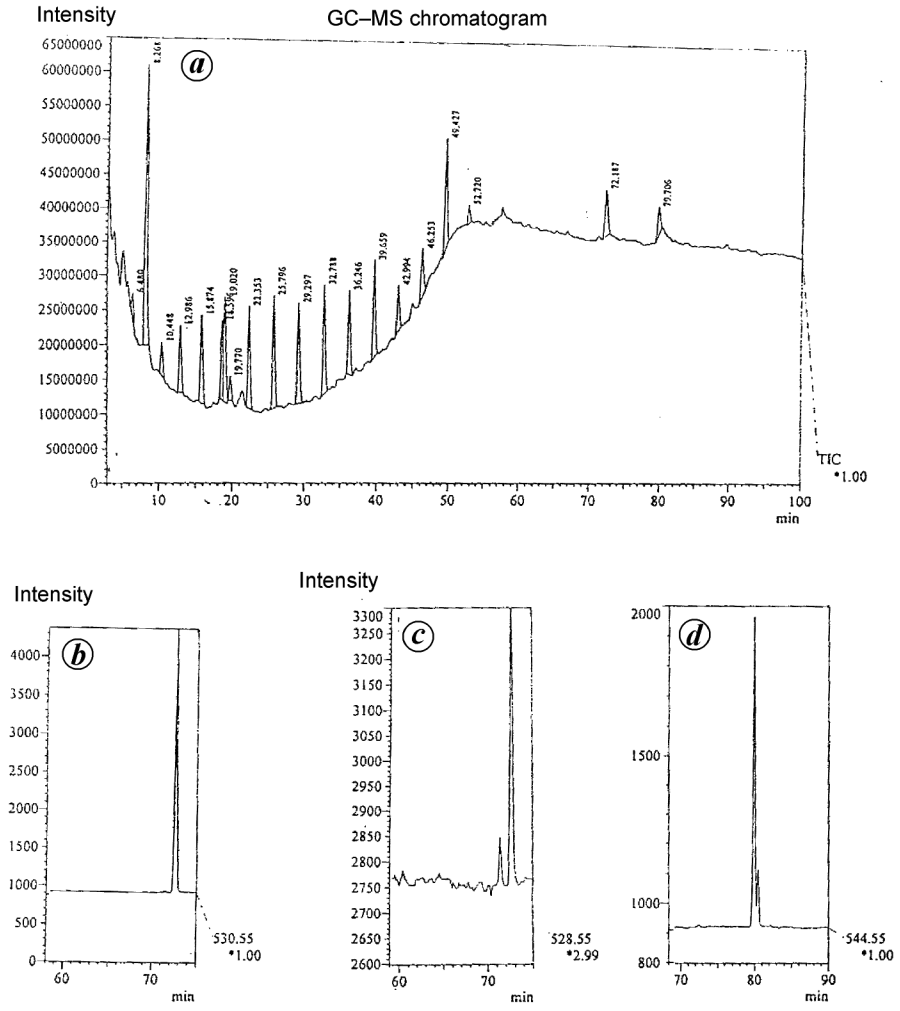


**Figure 1.** GC–MS chromatograms. ***a***, TIC (scan mode); ***b***, SIM (*m/z* = 530.55); ***c***, SIM (*m/z* = 528.55); ***d***, SIM (*m/z* = 544.55).

steps, including saponification that is intended to eliminate the interference of alkenoates, which also have similar retention times (RTs) like the alkenones we are looking for in GC[9]. For GC, the column used was HP-5 column, 30 m × 530 μm id with 0.88 μm film thickness. Temperature programming was 200–300°C @ 2°/min and held at 300°C for 40 min (total run time: 90 min) and the detector used was Flame Ionization Detector (FID) in split mode (2 : 1). The detector temperature was maintained at 320°C and helium was used as carrier gas. Hexatriacontane ($C_{36}H_{74}$) and nonadecanone ($C_{17}H_{35}COCH_3$) were used as gas chromatographic standards. Peaks of alkenones in sample chromatograms are similar in relative RTs and shapes to those presented in the literature[10,11].

Pure samples of LCA were not available with us for use as calibration standards. We relied on GC-MS (Shimadzu, QP 5050) for identification of the LCAs. The GC–MS in 'Total Ion Chromatogram (TIC)' mode of the 230 cm bsf (LGM) sectional sample in which the less abundant trienone is expected to be relatively enriched, is shown in Figure 1. Inspection of the peaks, including the longer RT peaks did not reveal *m/z* 530.55 and 528.52 ions corresponding to the molecular ions of dienone and trienone LCAs respectively. GC in the 'single ion mass' (SIM) mode[12], with these mass numbers alone selected separately at RTs 72.19 and 71.17 min respectively, did reveal the peaks. In the former spectrum (*m/z* 530.55), the peak at RT 72.19 min occurs alone. But in the latter (528.52), the (minor) peak at RT 71.17 min is associated with the erstwhile peak (72.19 min) of the dienone, assigned to the fragment ($M^+ - 2$). A third fragment at 544.55 corresponding to twin LCAs, viz. $C_{38:2}$ Et (major peak, RT = 80.014) and $C_{38:2}$ Me (minor peak, RT = 80.525)[10], is rather easily discernible in TIC as well as SIM spectra. The experiment on GC–MS was repeated on several test samples, yielding reproducible results.

In order to scale up our procedure for routine use, GC (with FID) was done on the same samples for which GC–MS were done using similar chromatographic conditions. The relative intensities of the dienone and trienone peaks

matched well with those in the GC–MS SIM spectra. SD in the ratio of the two peaks was ~ 5%. From the relative abundances (i.e. peak areas) of the di- and tri-unsaturated alkenones (in the gas chromatograms), the unsaturation index ($U^{K'}_{37}$) was calculated using eq. (1)[6].

Oxygen isotope ratios were determined on samples of surface-dwelling planktonic foraminifer, *Globigerinoides ruber* (white) at every 10 cm interval. Forty uniform tests of *G. ruber* (150–300 μm size fraction) from each sample, free from coloration were manually crushed in methanol and cleaned in an ultrasonic bath. The carbonate tests were reacted in saturated pyrophosphoric acid at 60°C in a vacuum system on-line to a Micromass (UK) Isoprime model mass spectrometer at the National Institute of Oceanography, Goa. The isotopic composition of the evolved $CO_2$ is reported in δ notation as per mil (‰), calibrated against NBS 19 ($\delta^{18}O = -2.2$‰ deviation from PDB). The precision of the stable oxygen isotope analysis is ± 0.08‰ NBS 19.

The core (78°35′E, 8°05.090′N; see Sarma *et al.*[8]) is from the outer Gulf of Mannar at a water depth of 1395 m between the Indian and Sri Lankan land masses, a high productive area in the western Bay of Bengal[13]. Peak values of $CaCO_3$ (~ 55%) occur at the time of the LGM; the mean value for the glacial sediments is ~ 50%, compared to the Holocene mean value of ~ 25% (Figure 2). The carbonate deposition rate of ~ 3.5 cm k $yr^{-1}$ in the Holocene sediment is preceded by a higher ~ 5 cm k $yr^{-1}$ around the LGM. Although $CaCO_3$ is an established productivity proxy, its concentration or deposition rate cannot always be taken so, for dilution by lithogenic inputs and dissolution, factors that change with time can greatly alter the seafloor $CaCO_3$ concentration, independent of surface water primary production. Organic carbon (OC) of sediments varied in the range of 4.0–1.5%, the glacial sections being poorer (mean: 2.5%) than the Holocene sections (3.9%). OC also suffers from uncertainties for use as a palaeoproductivity proxy due to the competing processes of productivity or lithogenic addition and degradation. LCAs are useful in such a scenario as they are dependable proxies of not only SST, but also surface productivity[14].

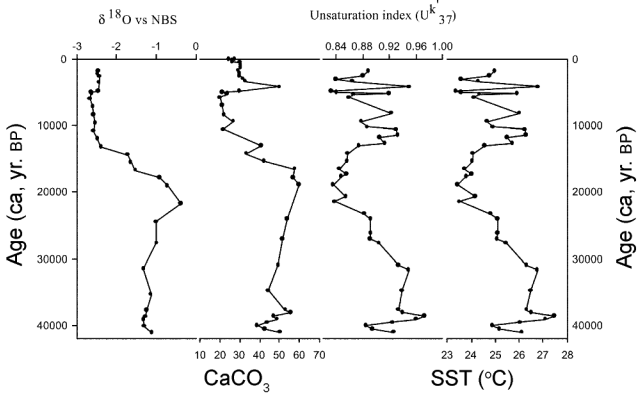


**Figure 2.** Downcore profiles of $\delta^{18}O$, $CaCO_3$, $U^{K'}_{37}$ and SSTs.

Difficulty in the recognition of molecular ions of the LCAs in the GC–EI MS TIC spectra is because the LCAs undergo extensive fragmentation under the strong electron impact of 70 eV at carbons α to the carbonyl and by β-cleavage at the double bonds[15]. Thus, fragments of *m/z* 43, 110, 206, 251, 347 and 487, in the order of decreasing abundances are noticed. Multiple cleavage modes make difficult the structural determination of long carbon chain ketones[16]. The formation of $(M^{+\cdot} - 2)$ fragment from the dienone (that has overlapped with trienone peak in the SIM mode GC at *m/z* 528.52) is shown in Scheme 1. The contribution of this ion to the TIC, calculated from the gas chromatograms was only *ca.* 2% of the molecular ion. However, it appears larger in the *m/z* 528.52 SIM spectrum as the concentration of dienone is much larger than trienone in the sample and because trienone undergoes more extensive degradation than dienone under electron impact. In the SIM mode, the quadrupole mass analyser, instead of trying to catch the infinite number of ions, would confine to the selected ion(s), thereby increasing the sensitivity multiple fold[12], and hence would be able to detect trienone and dienone at $M^+$ 528.52 and 530.55 respectively. The possible interference of co-eluting compounds (such as hydrocarbons) is also eliminated in this way, as their mass numbers being different are not detected in the SIM mode.

The yield of total lipid extract varies between 0.25 and 0.06% of the dry sediment (Figure 3). Although the glacial sections contain less OC and produced less extractable lipid, LCAs ($C_{37:3} + C_{37:2}$) as its fraction are thrice as large in glacial sediments compared to the Holocene sediments. Hence, glacial primary productivity may be interpreted as larger than the Holocene primary productivity[14]. Primary productivity is monsoon-dependent. The core site lies in an area influenced predominantly by the winter monsoon[17] that causes surface nutrient enrichment by convective currents. As the process was more efficient in the glacial phase, the primary production should have been higher then. Our alkenone data conform to this trend.

The alkenone unsaturation index (mean: 0.90) and the corresponding SSTs (mean: 25°C) calculated for the Holocene sediments are higher than for those around the LGM (0.84 and 23°C respectively; Figure 2). For the calculation of palaeo-SST from $U^{K'}_{37}$ values, we used the Prahl equation established for *Emiliana huxleyi* laboratory cultures[18] and used as the global standard: $U^{K'}_{37} = 0.034T + 0.039$. Sonzogni *et al.*[19], working on surface sediments from different regions of the Indian Ocean, (eastern) Bay of Bengal included, found little deviations from this equation. They proposed the equation for the flux-weighted annual mean (FWAM) SST as $U^{K'}_{37} = 0.034T + 0.013$, which yields calculated SSTs that are ~ 0.75°C higher than those obtained with the Prahl equation. Calculation of SST by both equations shows an identical glacial cool-

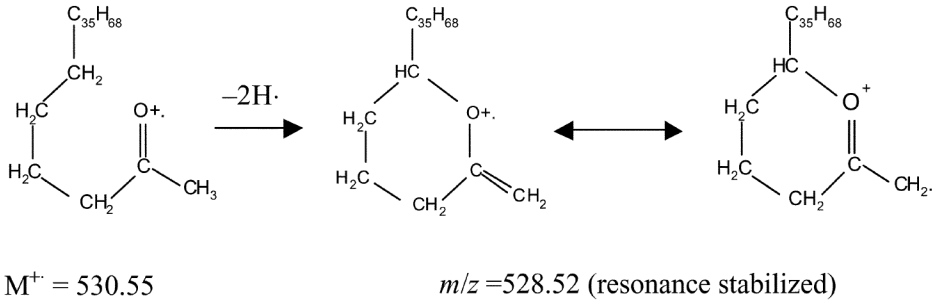


$M^{+\cdot} = 530.55$ $m/z = 528.52$ (resonance stabilized)

**Scheme 1.** Formation of $(M^{+\cdot} - 2)$ fragment ($m/z$ = 528.52) from dienone ($M^{+\cdot}$ = 530.55).

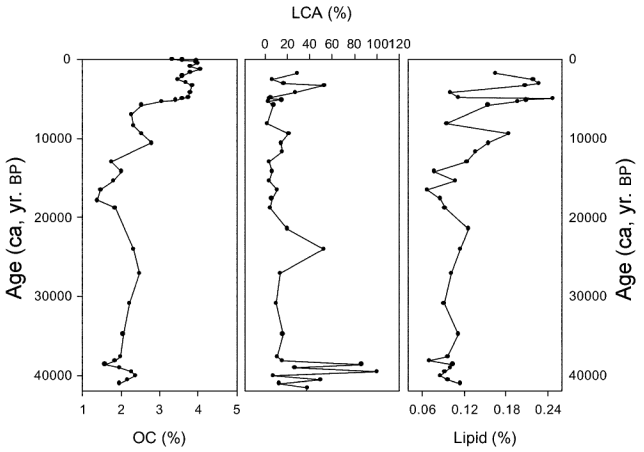


**Figure 3.** Organic carbon, relative yields of LCA fractions in lipid, and lipid yield of dry sediment.

ing of 2.75°C with respect to the Holocene, a result that is compatible with that reported for the tropical Indian Ocean[20] and eastern Arabian Sea[3,9].

Oxygen isotope records of the western Bay of Bengal are rare. A core from the nearest region where *G. ruber* has been studied is in the central Bay of Bengal (10°43′N, 90°27′E; water depth: 3246 m)[21], in which the glacial-to-interglacial $\delta^{18}O$ amplitude ($\Delta\delta^{18}O$) was ~ 2 per mil. To this amplitude, increased polar ice, ocean surface cooling and surface salinity were interpreted to contribute 1.2, 0.25 (corresponding to a glacial cooling of 1°C) and 0.55‰ (corresponding to a salinity increase of 2‰) respectively. In the present case, the $\Delta\delta^{18}O$ is 2.2‰. Since the original estimate of global ice contribution to $\delta^{18}O$ increase in the glacial with respect to the interglacial[22] of ~ 1.2‰ has been recently revised[23,24] as ~ 1.0‰, the residual $\Delta\delta^{18}O$ of as much as 1.2‰ is to be inferred as the combined contribution of cooling and salinity increase during the glacial. A 2.75°C cooling as shown above by the study of alkenone that can account for a $\Delta\delta^{18}O$ of ~ 0.65‰, still leaves behind 0.55‰ that can be accounted by a ~ 2‰ increase of salinity that was caused by low influx of Ganges–Brahmaputra (GB) water in the glacial time due to weakened SW monsoon at that time[7]. The salinity increase at the time of LGM is similar to that inferred at the central Bay of Bengal site[21]. Around the LGM, the alkenone index, a truer palaeo-SST indicator fell more rapidly than the rise in $\delta^{18}O$. Thus alkenone index emerges as a more dependable palaeo-SST (and productivity) proxy for the study area.


1. Rohling, E. J. and Cooke, S., Stable oxygen and carbon isotopes in foraminiferal carbonate shells. In *Modern Foraminifera* (ed. Sen Gupta, B. K.), Kluwer, Dordrecht, 1999, pp. 230–258.
2. Lea, D. W., Trace elements in foraminiferal calcite. In *Modern Foraminifera* (ed. Sen Gupta, B. K.), Kluwer, Dordrecht, 1999, pp. 259–277.
3. Bard, E., Comparison of alkenone estimates with other palaeotemperature proxies. *Geochem. Geophys. Geosyst.*, 2001, **2**, 2000GC000050.
4. Hoefs, M. J. L., Versteegh, G. J. M., Rijpstra, I. C., de Leeuw, J. W. and Sinninghe Damsté, J. S., Post-depositional oxic degradation of alkenones: implications for the measurement of palaeo-sea surface temperatures. *Paleoceanography*, 1998, **13**, 42–49.
5. Prahl, F. G., de Lange, G. J., Lyle, M. and Sparrow, M. A., Post depositional stability of long-chain alkenones under contrasting redox conditions. *Nature*, 1989, **341**, 434–437.
6. Prahl, F. G. and Wakeham, S. G., Calibration of unsaturation patterns in long-chain ketone compositions for palaeotemperature assessment. *Nature*, 1987, **330**, 367–369.
7. Rostek, F., Ruhland, G., Bassinot, F. C., Muller, P. J., Labeyrie, L. D., Lancelot, Y. and Bard, E., Reconstructing sea surface temperature and salinity using $\delta^{18}O$ and alkenone records. *Nature*, 1993, **364**, 319–321.
8. Sarma, N. S., Rama Krishna, M. S. and Pasha, Sk. G., Amino-stratigraphy of sediments of the SW Bay of Bengal. *Curr. Sci.*, 2003, **85**, 435–436.
9. Schulte, S. and Muller, P. J., Variations of sea surface temperatures and primary productivity during Heinrich and Dansgaard-Oeshger events in the northeastern Arabian Sea. *Geo-Mar. Lett.*, 2001, **21**, 168–175.
10. Brassell, S. C., Eglington, G., Marlowe, L. T., Pflaumann, U. and Sarnthein, M., Molecular stratigraphy: a new tool for climatic assessment. *Nature*, 1986, **320**, 129–133.
11. Schulte, S., Mangelsdorf, K. and Rullkotter, J., Organic matter preservation on the Pakistan continental margin as revealed by biomarker geochemistry. *Org. Geochem.*, 2000, **31**, 1005–1022.
12. Mcmaster, M. and Mcmaster, C., *GC/MS. A Practical Users Guide*, Wiley-VCH, 1998, pp. 1–161.
13. Verlecar, X. N. and Parulekar, A. H., Primary productivity. In *The Indian Ocean – A Perspective* (eds Sen Gupta, R. and Desa, E.), Oxford & IBH, New Delhi, 2001, vol. 2, pp. 397–416.

14. Prahl, F. G., Dymond, J. and Sparrow, M. A., Annual biomarker record for export production in the central Arabian Sea. *Deep-Sea Res.*, 2000, **47**, 1581–1604.
15. Hill, H. C., *Introduction to Mass Spectrometry*, Heyden & Son Ltd, 1966, pp. 1–135.
16. Beynon, J. H., Saunders, R. A. and Williams, A. E., The mass spectra of organic molecules, 1968, p. 508.
17. Sarkar, A., Ramesh, R., Bhattacharya, S. K. and Rajagopalan, G., Oxygen isotope evidence for a stronger winter monsoon during the last glaciation. *Nature*, 1990, **343**, 549–551.
18. Prahl, F. G., Muehlhausen, L. A. and Zahnle, D. L., Further evaluation of long-chain alkenones as indicators of palaeoceanographic conditions. *Geochim. Cosmochim. Acta*, 1988, **52**, 2303–2310.
19. Sonzogni, C., Bard, E., Rostek, F., Lafont, R., Rosell-Mele, A. and Eglinton, G., Core-top calibration of the alkenone index versus sea surface temperature in the Indian Ocean. *Deep-Sea Res.*, 1997, **44**, 1445–1460.
20. Sonzogni, C., Bard, E. and Rostek, F., Tropical sea-surface temperature during the last glacial period: a view based on alkenones in Indian Ocean sediments. *Quat. Sci. Rev.*, 1998, **17**, 1185–1201.
21. Ahmad, S. M., Carbon and oxygen isotopic records of planktonic and benthic foraminifera from a new deep sea core of the northeast Indian Ocean. *Curr. Sci.*, 1995, **69**, 691–695.
22. Shackleton, N. J., Oxygen isotopes, ice volume and sea level. *Quat. Sci. Rev.*, 1987, **6**, 183–190.
23. Schrag, D. P., Hampt, G. and Murray, D. W., Pore fluid constraints on the temperature and oxygen isotopic composition of the glacial ocean. *Science*, 1996, **272**, 1930–1932.
24. Shackleton, N. J., The 100,000-year ice-age cycle identified and found to lag in temperature, carbon dioxide, and orbital eccentricity. *Science*, 2000, **289**, 1897–1902.

ACKNOWLEDGEMENTS. We thank Prof. C. Subrahmanyam for kindly providing the GC–MS data and Mr V. V. S. Prasada Rao, who operated the instrument. Financial assistance from DOD, Govt. of India through a research project (to N.S.S.) and CSIR, New Delhi through SRFs (to Sk.G.P. and M.S.R.K.) is acknowledged.

Received 27 October 2005; revised accepted 4 March 2006

# ESR investigation of deferration treatment of iron-rich kaolinite clay from Deopani, Assam, India

**P. Sengupta*, N. J. Saikia, D. J. Bharali, P. C. Saikia and P. C. Borthakur**

Regional Research Laboratory (CSIR), Jorhat 785 006, India

**Kaolin, available at Deopani, Assam, India, is yet to be commercially exploited due to lack of detailed characteristics and appropriate process for beneficiation. The characteristics of the clay, as revealed by chemical, XRD, FTIR and SEM–EDX analyses and beneficiation by physico-chemical methods were reported earlier. The Fe content of the clay could be reduced considerably from a high value of 9.48 to 1.0% by adopting simple beneficiation techniques due to favourable Fe-mineralogical form, but it is difficult to remove the impurities completely. This communication reports the characteristics of the clay and its beneficiated products, as revealed by ESR investigation. The clay contains relatively high amounts of both structural and non-structural iron and minor amount of Mn. The *g* factors calculated from the ESR signals are used to investigate the effect of the beneficiation techniques employed on structural and non-structural Fe. Magnetic separation and size fractionation yield products with high amount of structural iron. Oxalic acid that acts both as a complexing and leaching agent at relatively low concentration preferentially leaches structural iron, and at higher concentration removal of non-structural iron is enhanced. Increase in temperature initially from ambient condition results in preferential removal of the non-structural iron and thereafter it becomes the same for both forms of iron.**

**Keywords:** Beneficiation, deferration, ESR spectra, kaolinite, structural and non-structural iron.

Many of the physical, chemical and thermal properties of clays are influenced by the presence and nature of impurities[1]. Iron, one of the most common impurities in kaolinite clays, may occur as part of the clay structure or as separate Fe-bearing phases. Both the types, termed as 'structural' and 'non-structural' iron respectively, usually coexist in kaolinite. Structural irons result from isomorphous substitution of both octahedral-Al and tetrahedral-Si in the kaolinite structure, whereas non-structural iron is due to the coatings and discrete iron-bearing phases present in clay[2,3].

Industries like ceramic, paper, paint, rubber, plastic, polymer, cosmetics, medicine, insecticide, pesticide, etc. widely use kaolinite clay for various purposes. Presence of iron-bearing impurities in kaolinite is detrimental to its use[1]. Several physical and chemical processes like sieving, magnetic separation[4], selective flocculation[5], ultrasound cleaning[6], leaching with chemicals like oxalic and other organic acids[7,8], organic acids in the presence of a fermented medium[9], lixiviant containing microbially-produced oxalic and hydrochloric acid[10], carbohydrates[11], EDTA[12], sodium dithionate–$H_2SO_4$ mixtures[13,14], etc. have been employed to lower the iron content of clay. The residual iron after the deferrating treatments may exist either as structural and/or non-structural type[3,15,16].

Several kaolin (china clay) deposits have been located in Northeast India, including the one at Deopani, Karbi Anglong district, Assam. None of these deposits have been commercially exploited due to lack of detailed characteristics and appropriate processes for beneficiation. We had earlier reported the location and content of the deposit, characteristics of the clay as revealed by chemical, XRD, FTIR and SEM–EDX analyses and beneficiation

*For correspondence. (e-mail: pinakiajitsengupta@yahoo.com)